

INVESTIGATION OF TRANSITION MODELLING FOR AEROFOIL DYNAMIC STALL

J. L. Hill and S. T. Shaw

Department of Aerospace Sciences, School of Engineering, Cranfield University,
Cranfield, United Kingdom

N. Qin

Department of Mechanical Engineering, Sheffield University
Sheffield, United Kingdom

Abstract

A method for computing low Reynolds number flows containing laminar-turbulent transition is described. The model employs empirical relationships to describe the onset and extent of transition and is coupled with a two equation turbulence model. Results are presented for two aerofoil configurations that demonstrate the ability of the model to compute attached transitional flows and flows involving leading edge separation. The model is used to investigate transitional flows on aerofoils performing unsteady pitching motion.

Introduction

Dynamic stall occurs on any manoeuvring lifting surface whose effective angle of attack exceeds the normal static stall angle. The basic phenomenological aspects of dynamic stall are described for aerofoils and rectangular wings by Carr [1]. For pitching aerofoils the sequence of events, see Figure (1), is initiated by the development of a leading edge vortex as the aerofoil pitches above the static stall angle of attack. The developing vortex increases the lift generated by the aerofoil. As incidence increases further the vortex separates from the leading edge and is convected downstream over the aerofoil surface. This vortex movement is responsible for rapid changes in both magnitude and sign of pitching moment. Lift stall occurs as the vortex moves downstream of the trailing edge. Generally the boundary layer remains separated over much of the down stroke reattaching as the aerofoil approaches its minimum incidence. The boundary layer is normally fully attached at the end of the down stroke.

Dynamic stall phenomena are important in many fields of aerospace science including turbo-machinery, wind turbines and manoeuvring fixed wing aircraft. In rotorcraft engineering a detailed understanding of the unsteady airloads acting on the moving blades is essential for the prediction of rotor performance, rotor dynamics (including blade aero-elastics) and noise generation in forward flight.

Much of our understanding of dynamic stall has come through careful experimentation on single element

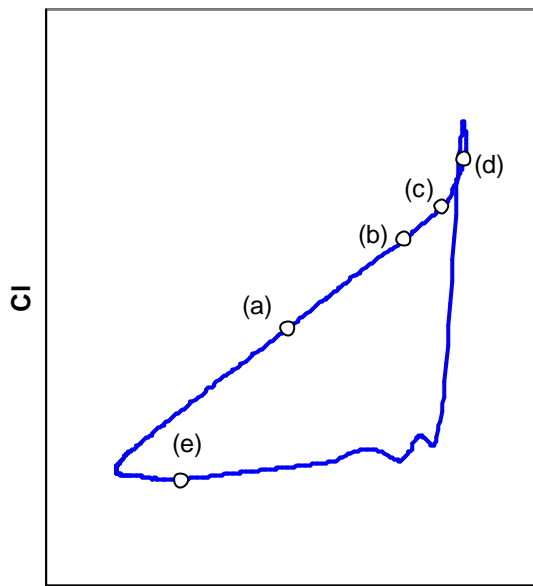
aerofoil configurations using pitching oscillations to generate the required unsteadiness. Reviews of progress in the experimental understanding of dynamic stall phenomena have been presented by Carr [1] and Carr and Chandrasekhara [2].

The complex nature of the phenomena has led to a range of predictive models ranging in fidelity from simple empirical models to large eddy simulations. Semi-empirical models, such as those used by Westland Helicopters [3] provide robust practical tools that can be used within the design environment. More recently rapid progress has been made in the application of numerical simulation tools to the problem of dynamic stall, see for example the reviews by Ekaterinaris [4] and [5].

The occurrence and progression of dynamic stall is sensitive to a number of parameters such as pitch rate, geometry, Mach number, amplitude and Reynolds number. Numerical methods based upon the solution of the Navier-Stokes equations generally reproduce the qualitative behaviour of the flow with respect to such parameters. For dynamic stall initiated as a result of trailing edge acceptable quantitative agreement can generally be obtained with the experimental data for all but the most severe separations using modern one- and two-equation turbulence models.

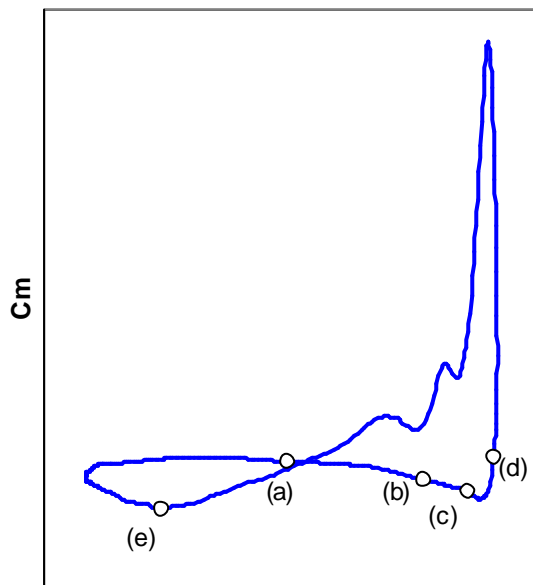
Quantitative agreement for stall initiated at the leading edge is less favourable. There is good experimental and numerical evidence, see for example the discussions of References [4] and [5] that in this case the flow is sensitive to the state of the boundary layer (laminar, transitional or fully turbulent) immediately ahead of the separation point.

Inclusion of transition within simulations based upon solution of the Reynolds averaged Navier-Stokes equations is challenging. Transition physics, mathematical tools for boundary layer stability analysis and progress made in transition prediction were reviewed by Malik [6] who identified four instability modes, Tollmien-Schlichting, Gortler, cross-flow and Mack. The relative importance of the individual instability modes for pitching aerofoils and wings is poorly understood. For pitching two-dimensional aerofoils only the Tollmien-Schlichting instability is relevant.



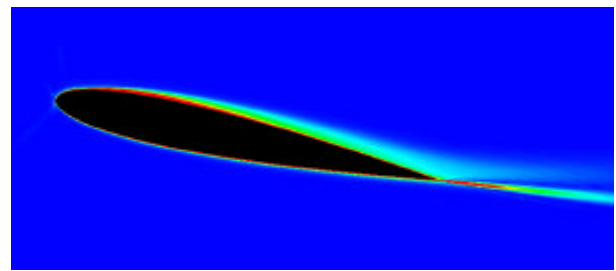
Incidence

(i) Normal Force Hysteresis

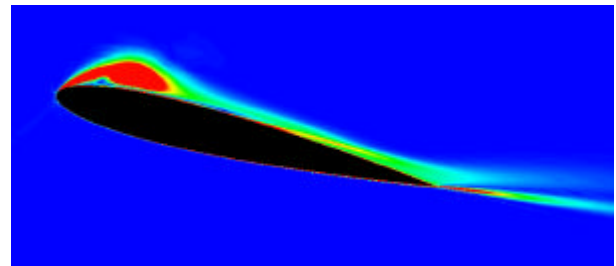


Incidence

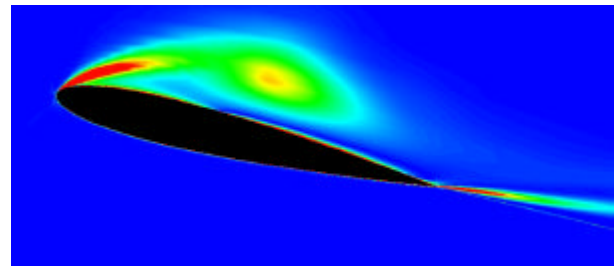
(ii) Pitching Moment Hysteresis



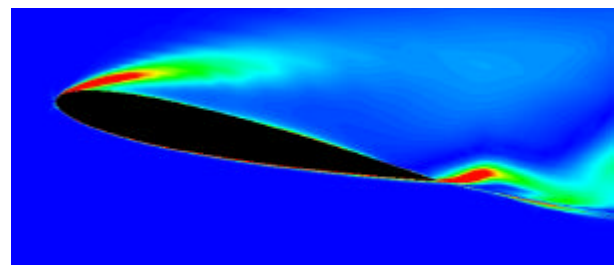
(a) Attached Flow



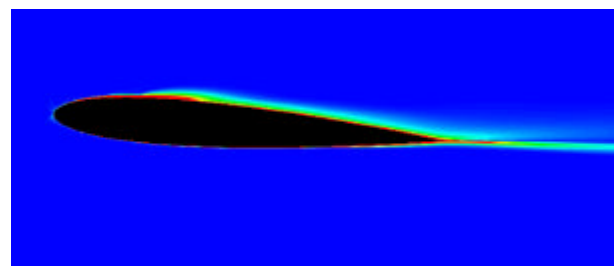
(b) Formation of Leading Edge Vortex



(c) Movement of Leading Edge Vortex



(d) Full Stall



(e) Re-attachment during Down Stroke

Figure (1): Dynamic Stall Events

Cebeci [7] highlighted the basic ingredients required to incorporate transition within Reynolds averaged Navier-Stokes simulations. These are the determination of transition onset, the length of transition and the modifications to the turbulence model to accommodate the presence of the laminar and transitional flow regimes. The latter has commonly been achieved by direct manipulation of the turbulent viscosity while two alternate strategies, empiricism or stability analysis, for the prediction of transition onset and extent can be identified.

Ekaterinaris and his co-workers [4,5,8] employed empirical models for transition onset, namely, Michel's criterion [9], and solutions of the thin-layer Navier-Stokes equations to study the development of laminar separation bubbles on a NACA 0012 aerofoil. Comparisons of the computed data with pressure distributions derived from optical measurements show that inclusion of a representation of the transition physics is crucial to improving predictive capability.

In this paper we review the engineering model developed by Hill, Shaw and Qin [10] for prediction of transition on aerofoils and rotating wings and apply the model to the attached and separated flows generated by oscillating aerofoils.

2. Numerical Method

The governing equations are the Reynolds-averaged Navier-Stokes equations together with the $k-\omega$ turbulence model described by Wilcox [11]. These equations can be written in the integral-conservation form,

$$\int_{\Omega} Q d\Omega + \int_S \vec{F} \cdot \vec{n} dS = \int_{\Omega} \vec{H} d\Omega \quad (1)$$

in which Q is the vector of conserved variables, \vec{F} is the flux function, \vec{n} is the outward pointing unit vector normal to the volume surface and \vec{H} is a source term arising from the turbulence model. The fluid is assumed to be a Newtonian perfect gas and Sutherland's law is employed to model the coefficients of viscosity and thermal conduction.

Spatial discretization of the governing equations is performed using a nominally third-order accurate Godunov scheme based upon the approximate Riemann solver described by Osher and Solomon [12]. The viscous fluxes are evaluated using a second-order finite volume approach in which derivatives are evaluated using Gauss's theorem.

The discretized equations are marched in time using a closely coupled implicit method in which the mean flow and the turbulent flow equations are solved simultaneously. Local time-stepping is utilized to accelerate convergence to the steady state for steady problems while a second order time accurate method

based upon the pseudo-time approach is utilized for time-dependent calculations.

This method has proven to be accurate, efficient and robust for a wide class of problems, see for example [13],[14],[15] and [16].

3. Transition Model

In order to accommodate the presence of transitional flow regime in the current calculations a transition model is employed. The transition model consists of three key elements; prediction of transition onset, prediction of the transition length and a method for using this information to control the behaviour of the turbulence model.

3.1 Transition Onset

The empirical criteria reported by Michel [9] are used in the present work to describe the location of transition due to the growth of Tollmien-Schlichting instabilities. In this model transition is assumed to occur when the local Reynolds number based upon the momentum thickness exceeds a critical value determined by the equation,

$$Re_{q,tr} = 2.9 Re_{x,tr}^{0.4} \quad (2)$$

in which Re_q and Re_x are the local Reynolds numbers based on momentum thickness and distance from the aerofoil leading edge respectively. The model requires knowledge of both the velocity at the boundary layer edge and the boundary layer momentum thickness.

Calculation of Momentum Thickness

The parameters employed in Michel's empirical model are those corresponding to a laminar boundary layer. Unfortunately this data may not be readily available from the Navier-Stokes solution. The basic problems are illustrated in Figure (2), which shows calculated distributions of Reynolds number based on momentum thickness for two-boundary layers tripped at different chord-wise locations (12% and 20% chord).

As expected, Figure (2) shows a rapid growth in momentum thickness immediately following the onset of transition, reflected in a near instantaneous change in gradient of the curve. This behaviour has the effect of inhibiting the movement of the transition point aft of the initial transition location into the transitional region as the solution converges towards a steady state. In addition, there is evidence of upstream influence of the transitional and fully turbulent flow regimes, which may produce non-trivial changes in the computed boundary layer upstream of the transition location. These problems may lead to erroneous predictions of transition off set when the method is used interactively for steady flow computations

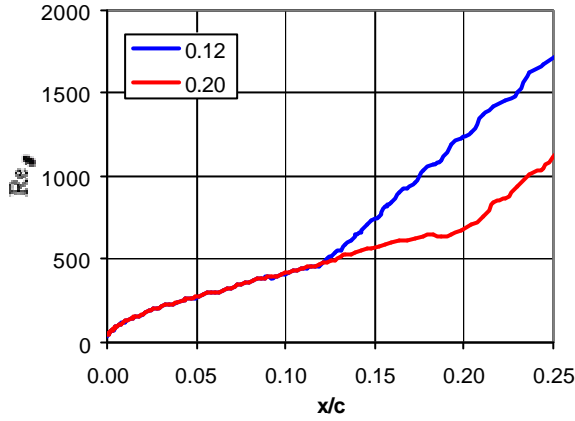


Figure (2): Computed behaviour of Reynolds number based on momentum thickness following transition to turbulent flow

or when used to model the boundary development on moving surfaces.

In order to overcome these problems it is necessary to model the behaviour of an *equivalent* laminar boundary layer using information from the Navier-Stokes solution. In the present work this is achieved using Thwaites method [17] in which the development of the local momentum thickness for an incompressible is related to an integration of the velocity distribution at the boundary layer edge,

$$q(x)^2 \approx \frac{0.45u}{u^6} \int_0^x u^5 dx \quad (3)$$

In order to predict transition using Michel's method we now require only the velocity distribution along the edge of the boundary layer from the CFD solution.

Determination of velocity distribution

Although the complete velocity field is known at each iteration of the time marching procedure the edge of the boundary layer is generally ill-defined. This problem is evident from the irregularity of the predicted momentum thickness distributions shown in Figure (2).

For incompressible potential flows the relationship between the external pressure distribution and the velocity along the boundary layer edge can be expressed through,

$$u = U_\infty \sqrt{1 - C_p} \quad (4)$$

If we further assume that the boundary layer is thin then from boundary layer theory we have,

$$\frac{\partial P}{\partial y} = 0 \quad (5)$$

which in conjunction with (4) allows the velocity distribution along the boundary layer edge to be related directly to the surface pressure distribution?

Adoption of this procedure provides significant advantages over direct computation that greatly improve the reliability and robustness of the method. In contrast to the boundary layer profiles the pressure distribution converges rapidly to the final solution. Furthermore, the surface pressure distribution is relatively insensitive to the choice of grid

Separation Model

Michel's criterion applies to attached laminar boundary layers with and without pressure gradient. The model fails for flows involving laminar separation. The current method is extended to deal with the possibility of a laminar region through the use of a separation model. While Krumbeins' [18] model, in which transition is fixed at the laminar separation point, is easy to implement it generally predicts transition ahead of the expected location. Several empirical models for transition within separation bubbles have been reported in the literature. In the present work we employ the model described by Schmidt [19],

$$x_{tr} = \frac{2175}{u_s} q_s^{0.5150} \quad (6)$$

in which the location of transition is related to the momentum thickness based on distance from the separation point.

3.2 Extent of the Transition Region

The extent and intermittency in the transition region are evaluated using the empirical model presented by Walker [20]. In this model the length of the transition regime is determined from the solution of,

$$Re_{l_{tr}} = 5.2 \left(Re_{\frac{x}{x_{tr}}} \right) \quad (7)$$

and the intermittency is determined from,

$$c(x) = 1 - e^{-4.65 \left(\frac{x - x_{tr}}{l_{tr}} \right)} \quad (8)$$

Forward of the predicted transition location the intermittency is set to,

$$c(x)=0 \quad x < x_{tr} \quad (9)$$

while aft of the transition region intermittency is given by,

$$c(x)=1 \quad x > x_{turn} \quad (10)$$

3.3 Modification Turbulence Model

Wilcox [21] has shown that low Reynolds number formulations of the $k-\omega$ turbulence model are capable of predicting transition like phenomena in the absence of an explicit transition model, see for example Figure (3), which shows computed contours of the turbulent Reynolds number Re_T obtained using the low Reynolds number without transition model. This capability is achieved through attenuation of the production of turbulent kinetic energy and specific dissipation by the low Reynolds number model terms. The predicted location of transition is generally far aft of the measured location. Manipulation of the freestream boundary conditions can improve predicted transition location dramatically but this is at the expense of incorrect boundary layer development at the lifting surface.

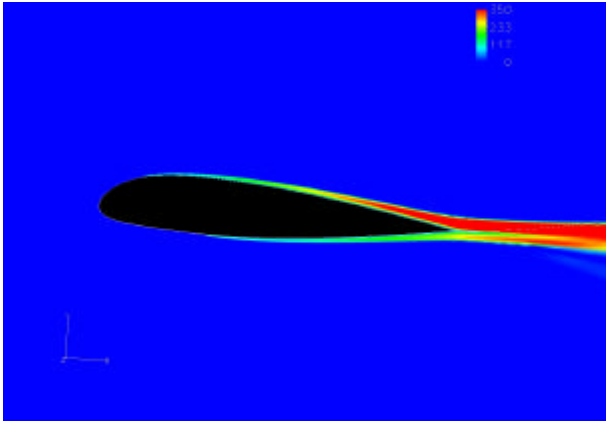


Figure (3): Contours of turbulent Reynolds number obtained using Wilcox Low Reynolds Number turbulence model

In order to accommodate the presence of the laminar and transitional regions in the current computations we adopt a similar, if less rigorous, approach in which the production terms appearing on the right-hand side of Equation (1) are attenuated by the calculated intermittency. Thus the production terms are calculated from,

$$\begin{aligned} P_k &= cP'_k \\ P_w &= cP'_w \end{aligned} \quad (11)$$

where the use of ' indicates the unmodified term and the intermittency is provided by Equations (8)-(10).

4. Steady Results

Results are first presented for steady two-dimensional flows over the NACA 0012 and Aerospatiale A- aerofoils at low Reynolds numbers. These computations provide an opportunity to assess the performance of the model for flows involving transition due to the growth of Tollmien-Schlichting instabilities and laminar separation.

The calculations were performed on structured grids which were adapted to the computation of boundary layer flows. Numerical experiments demonstrate that the present computations presented are grid converged.

4.1 NACA 0012 Aerofoil (High Reynolds Number)

Calculations were initially performed for a NACA 0012 aerofoil at a Reynolds number of $Re_c = 2,900,000$ and a freestream Mach number of $M = 0.15$, this corresponds to the experiment of Gregory [22]. The transition model was used in an interactive fashion, i.e. the transition location was updated at each iteration of the time marching procedure. Computed and measured transition locations are compared in Figure (4).

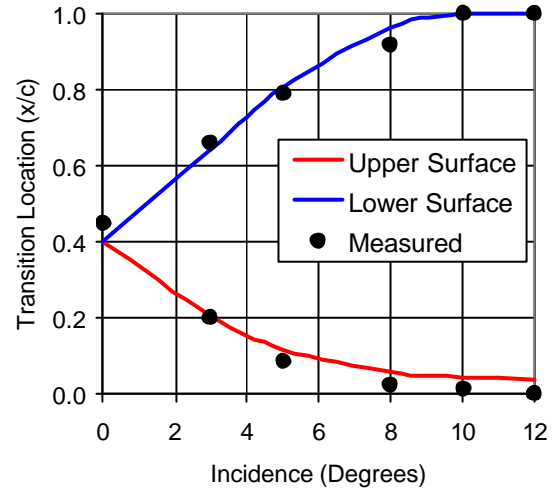


Figure (4) Comparison of computed and measured transition locations for NACA 0012 aerofoil $M = 0.15$ and $Re_c = 2,900,000$

For the incidence range considered transition on both the upper and lower surfaces is initiated by Michel's criterion (TS mode). Agreement between the computed and measured data is considered good at lower incidence. At higher incidence the computed transition location is generally aft of that measured in the experiment but the predictions remain acceptable.

4.2 NACA 0012 Aerofoil (Low Reynolds Number)

More recently detailed measurements of the low Reynolds flow over a NACA 0012 aerofoil have been performed by Favier and his co-workers at LABM; see for example references [23] and [24]. Detailed boundary layer measurements were taken for both steady and unsteady (oscillating in pitch) flows which included records of the onset and completion of transition.

Here we consider the steady flow at a Reynolds number of $Re_c = 100,000$ and a Mach number of $M = 0.15$ over the incidence range studied experimentally. Figure (5) compares the computed location of transition onset and completion with the measured data.

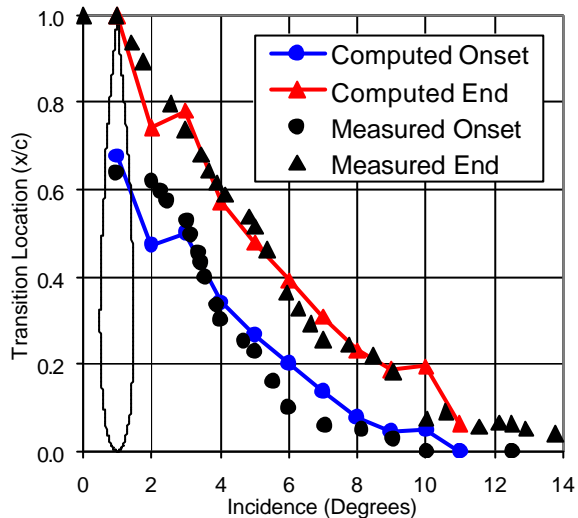


Figure (5) Comparison of computed and measured upper surface transition locations for NACA 0012 aerofoil $M = 0.15$ and $Re_c = 100,000$

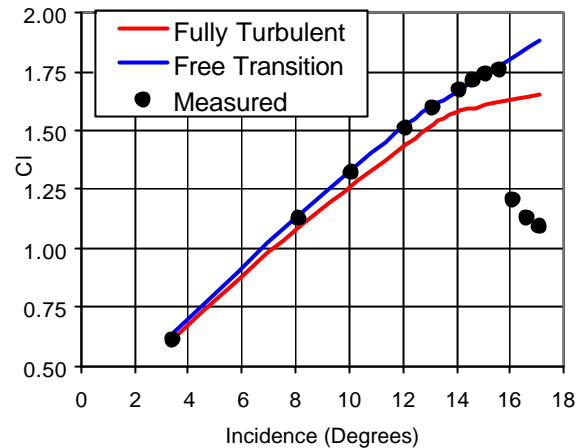
Comparison of the computed and measured data is considered fair. The computations indicate the presence of laminar separation and turbulent re-attachment over much of the incidence range. At low incidences the separation is towards the mid-chord but moves forward as incidence is increased. For a narrow range of incidences (4° to 8°) the flow remains fully attached and transition is initiated through the Tollmien-Schlichting instability mode. Beyond 8° of incidence, separation (and consequently transition) occurs close to the leading edge.

Results from fully turbulent calculations at this Reynolds number and Mach number indicate that the flow remains fully attached below 8° of incidence. Above this angle separation occurs, but in contrast to the free transition simulations separation is initiated at the aerofoil trailing edge and moves forwards as incidence is increased further. This contrast in physical behaviour between results obtained from the fully turbulent and free-

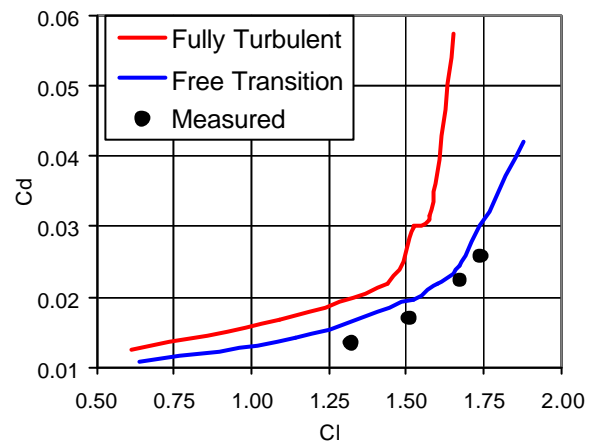
transition simulations illustrates the importance of modelling transition physics at lower Reynolds numbers.

4.3 A-Aerofoil

The final two-dimensional test case relates to the flow around the Aerospatiale A Aerofoil. This aerofoil has been the focus of an extensive European CFD validation effort [25]. Measurements include surface pressure coefficients, skin friction distributions and detailed boundary layer measurements.



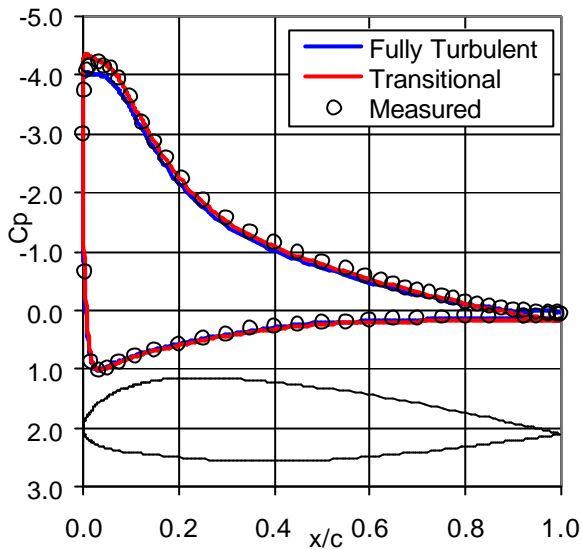
(a) Variation of lift coefficient with incidence



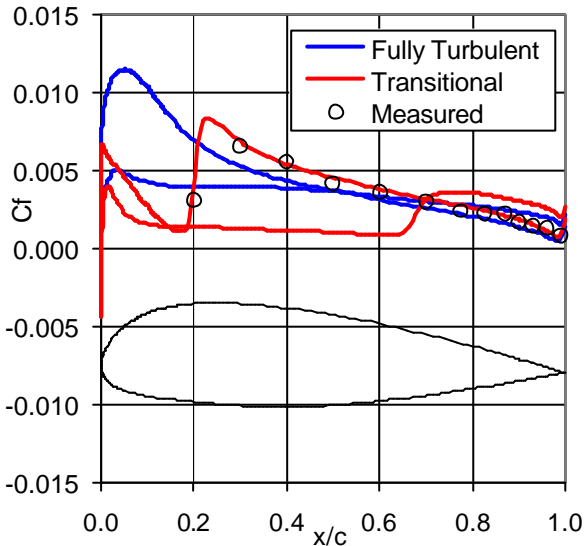
(b) Lift - Drag Polar

Figure (6) Comparison of fully turbulent and transition free computations Aerospatiale A-aerofoil $M = 0.15$ and $Re_c = 3,130,000$

Computations were performed for two Reynolds numbers, $Re_c = 3,130,000$ (F1) and $Re_c = 2,000,000$ (F2) and a Mach number of 0.15 on the common fine grid provided in [25]. This grid contains 513 points around the aerofoil and 129 in the direction normal to the surface.



(a) Pressure distribution



(b) Skin friction distribution

Figure (7) Comparison of fully turbulent and transition free computations Aerospatiale A-erofoil $M = 0.15$ and $Re_c = 3,130,000$

The variations of lift with incidence from fully turbulent calculations and free transition calculations are compared with experimental measurements at a Reynolds number of 3,130,00 in Figure 6). Also shown are the corresponding lift-drag polars. Use of the transition model improves agreement between the experimental and calculated lift coefficient significantly with excellent agreement observed between the computed and measured data over much of the incidence range. Use of the model also improves agreement between the computed and

measured drag coefficients although such comparisons remain poor.

Figure (7) is typical of the improvements between calculated and measured pressure and skin friction distributions that can be achieved using the present model. Improvements in computed pressure coefficient are generally confined to the leading edge region where significant improvements in the prediction of the leading edge suction are evident. This observation is the principal reason for improvements in computed lift coefficient. Comparisons of computed and measured skin friction distribution suggest that the transition location is well predicted (transition location was not measured in the experiment). The resulting reduction in skin friction in the leading edge region provide an explanation for the reduction in drag coefficient observed between fully turbulent and transition free calculations.

5. Unsteady Results

5.1 Attached Flow

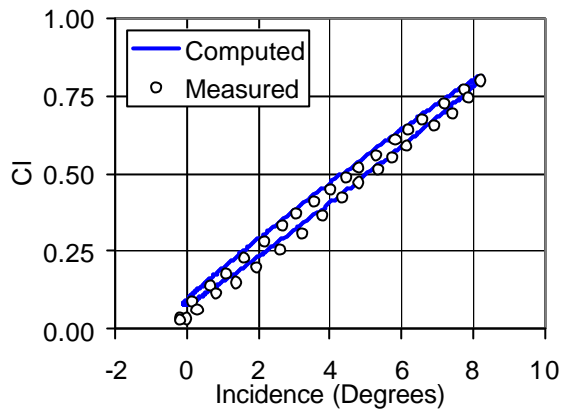
Initial calculations were performed to assess the ability of the numerical method to predict steady attached flows. Computations were performed for a NACA 0015 aerofoil performing pitching oscillations about the quarter-chord location at a Mach number of $M = 0.30$ and a Reynolds number $Re_c = 2,000,000$. The instantaneous incidence is determined from,

$$a(t) = 4.0 + 4.2 \sin(0.1t)$$

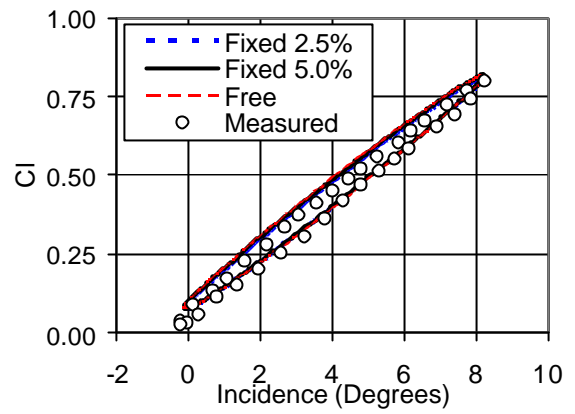
where t is a non-dimensional measure of time. This motion corresponds to the experiment of Pizzali [26].

The computed flow is attached over the full cycle. Computed hysteresis loops for lift, drag and pitching moment coefficients obtained assuming fully turbulent flow are compared with the measurements of Pizzali in Figure (8). The computed data were obtained by integration of the instantaneous pressure distributions at each time step. The agreement between the current calculations and the experimental data is generally favourable.

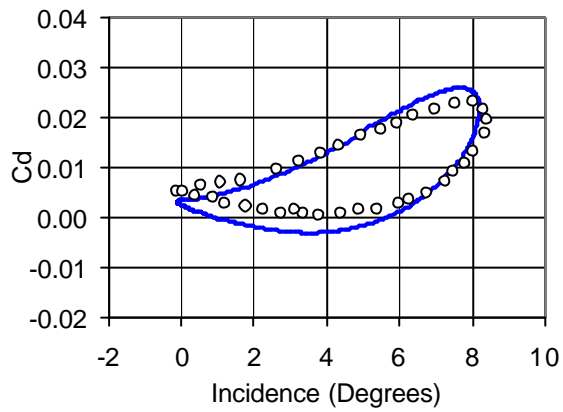
Calculations performed with transition fixed at 2.5% and 5.0% of the aerofoil chord and using the transition model are shown in Figure (9). The inclusion of transition in the computations has a small influence on the predicted lift and drag hysteresis. The differences are small during the upstroke and more significant during the downstroke. The corresponding improvements in pitching moment, Figure (9b) are much larger. Using the transition model leads to non-trivial improvements during the upstroke. There is also a general improvement during the downstroke compared to the results obtained assuming fully turbulent flow. It is believed that these differences occurs as a result of changes in the flow behaviour on the lower



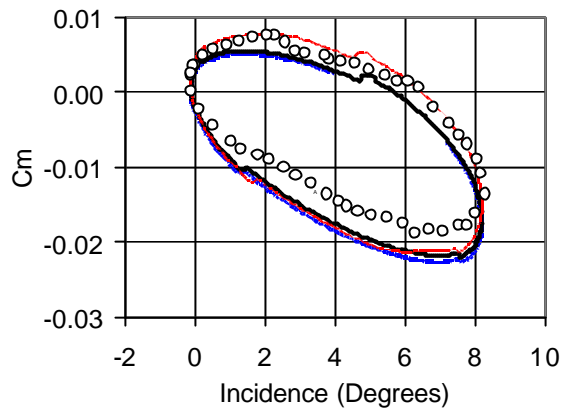
(a) Lift Coefficient



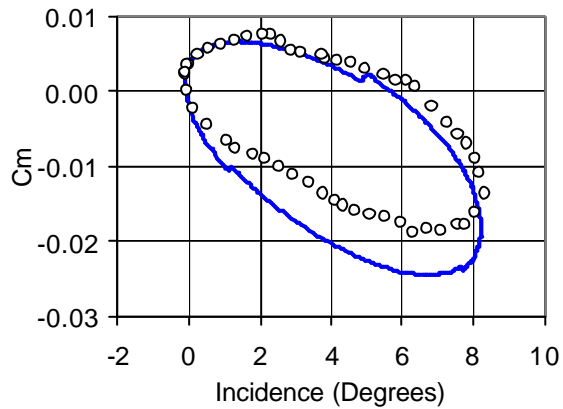
(a) Lift Coefficient



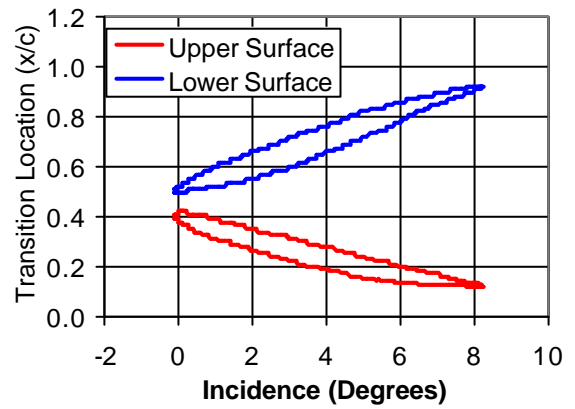
(b) Drag Coefficient



(b) Pitching Moment Coefficient



(c) Pitching Moment Coefficient



(c) Transition Location

Figure (8) Comparison of computed and measured forces and moments for pitching aerofoil (fully attached turbulent flow)

Figure (9) Comparison of computed and measured forces and moments for pitching aerofoil (fully attached transitional flow)

surface of the aerofoil, this leads to much better predictions of the shape of the instantaneous pressure distribution with obvious implications for the integrated forces and pitching moment.

The predicted transition locations are presented in Figure (9c). There is significant hysteresis on both the upper and lower surfaces. Transition on the aerofoil upper surface ranges from around 12% of chord at the beginning of the up stroke to 40% of chord at the beginning of the down stroke. Comparing the upper surface transition location during the up stroke and down stroke it is observed that at constant instantaneous incidence transition occurs earlier during the up stroke than during the down stroke. This is attributed to the action of the aerofoil acceleration and induced effects of the shed wake on the local pressure gradients.

5.2 Separated Flow

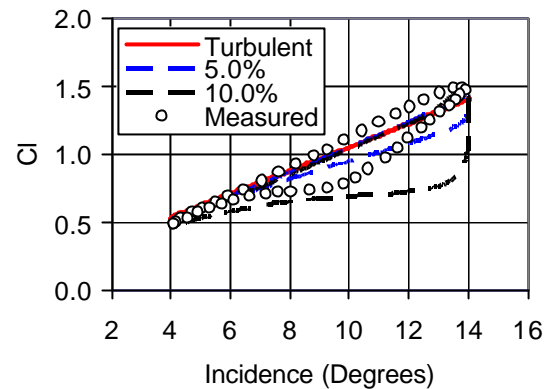
The effect of laminar/turbulent transition on dynamic stall predictions was investigated for a NACA 0012 aerofoil performing pitching oscillations about the quarter-chord location at a Mach number of $M = 0.30$ and a Reynolds number $Re_c = 4,000,000$. The instantaneous incidence was determined from,

$$a(t) = 9.0 + 5.0 \sin(0.1t)$$

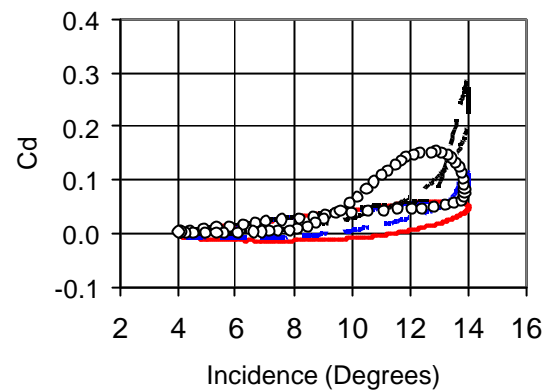
This motion corresponds to the experiment of McCroskey [27]. Initial computations were performed with transition fixed at the leading edge (fully turbulent) and at 5% and 10% of the aerofoil chord. The computed forces and moments are compared with the experimental measurements in Figure (10).

Figure (10) shows that fully turbulent computations are unable to reproduce all of the hysteresis effects observed in the experimentally measured forces and moments. This deficiency is particularly evident in the computed lift coefficient. This behaviour is attributed to the failure of the computation to resolve the flow break down at the leading edge correctly.

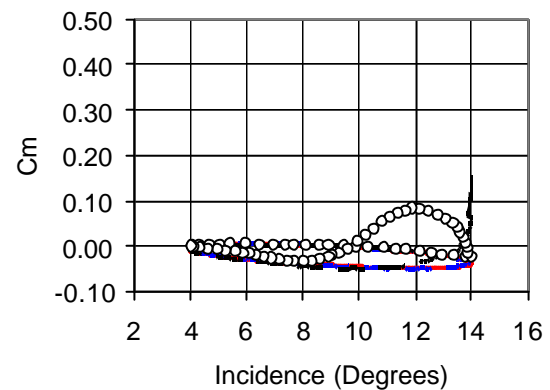
For computations performed with fixed transition close to the leading edge the complexity of the experimental hysteresis is observed in the computed data although quantitative agreement is poor. This is clearly evident in the computed lift coefficient data which indicate that movement of the transition location further aft results in increasingly heavy stall. Comparing the results of the fully turbulent and fixed transition computations it is evident that state of the boundary layer close to the leading edge plays an important role in the subsequent stall development. Examination of the computed pressure distributions supports this view. In the case of the fully turbulent calculation the leading edge pressure peak is maintained during the whole motion cycle, while in the fixed transition calculations the leading edge pressure



(a) Lift Coefficient



(b) Drag Coefficient



(c) Pitching Moment Coefficient

Figure (10) Influence of fixed transition on computed forces and moments for pitching aerofoil (fully attached transitional flow)

collapses during the down stroke indicating laminar separation. The extent and severity of this separation is determined by the transition location.

Subsequent computations were performed for this case using elements of the transition model described earlier. Results obtained using Michel's transition criteria and Walker's description of intermittency are presented in Figure (12). The corresponding transition locations are shown in Figure (11).

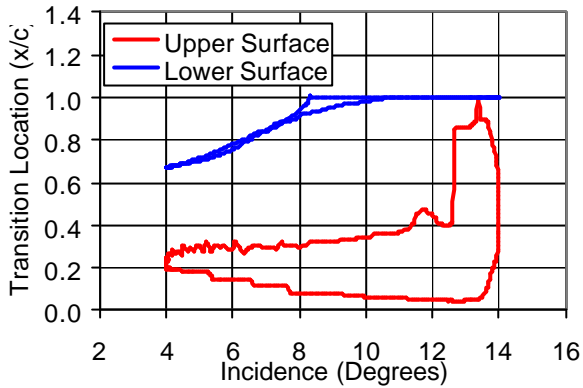
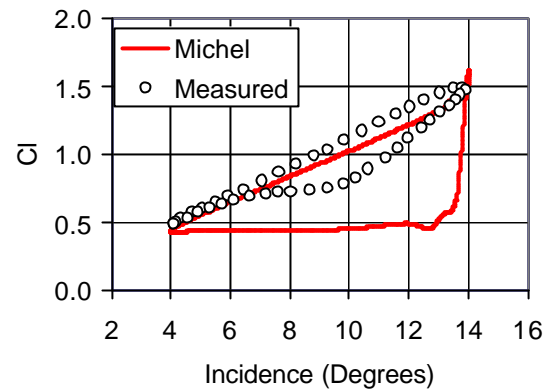


Figure (11) Predicted transition location for pitching aerofoil (fully attached transitional flow)

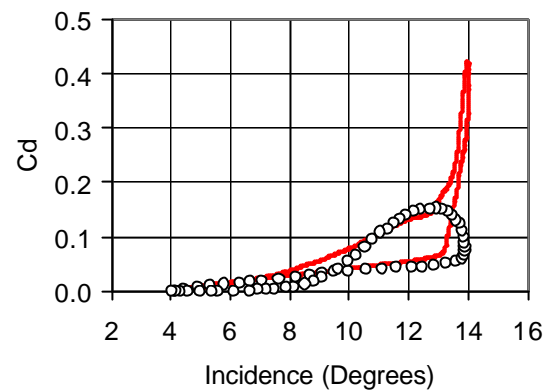
The predicted upper surface transition location remains close to the leading edge during the up stroke. Following the formation and separation of the dynamic stall vortex the transition location moves towards the trailing edge. Indeed early in the down stroke the upper surface transition location moves to the aerofoil trailing edge. The importance of the aerofoil pressure distribution in determining the boundary layer profiles employed in the Michel criteria, Equation (4), is responsible for this erroneous behaviour which arise as a consequence of the collapse of the leading edge pressure following stall, see for example Figure (14).

The importance of the length model was investigated. Calculations were performed using the Michel criteria with prescribed transition lengths of 1.25%, 2.5% and 5.0% of the aerofoil chord. The results of these calculations are compared with experiment in Figure (13). Results obtained with fixed transition lengths of 2.5% and 5.0% of aerofoil chord show similar behaviour to the fully turbulent calculations. Although they reproduce the complex hysteresis the stall is generally much heavier than observed in the experiment.

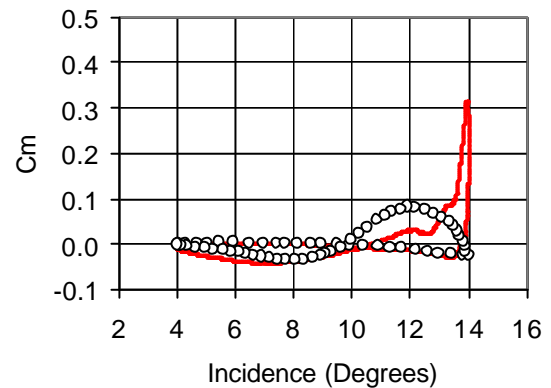
For the shorter transition length, 1.25% of aerofoil chord, quantitative agreement between the experimental and computed data is much improved. In an effort to better understand this behaviour a final calculation was performed without the use of the length model. Instead the



(a) Lift Coefficient

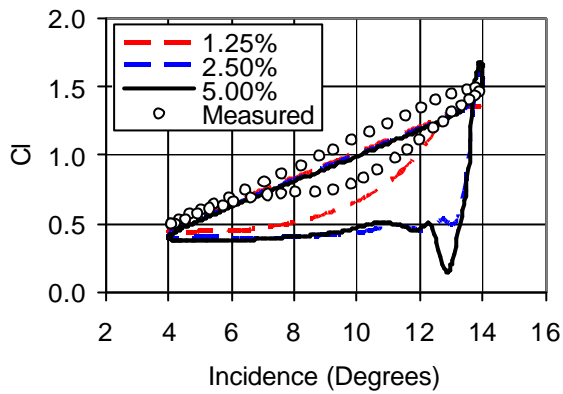


(b) Drag Coefficient

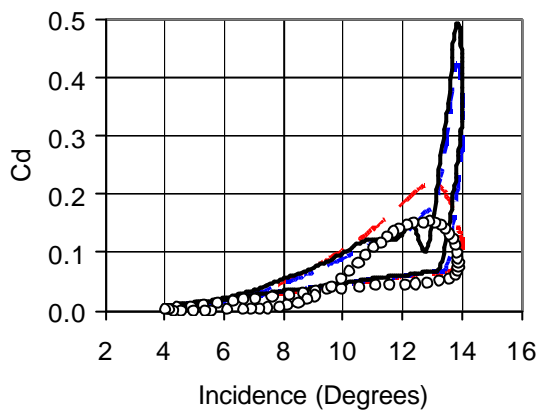


(c) Pitching Moment Coefficient

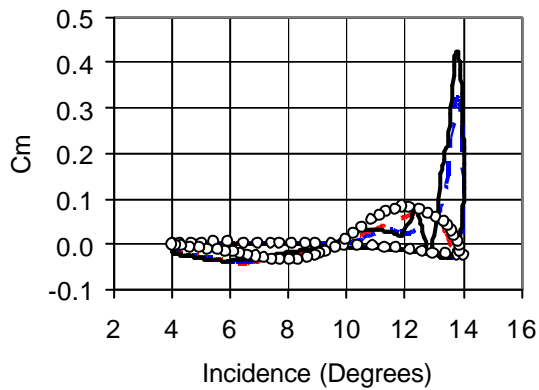
Figure (12) Influence of free transition on computed forces and moments for pitching aerofoil (fully attached transitional flow)



(a) Lift Coefficient

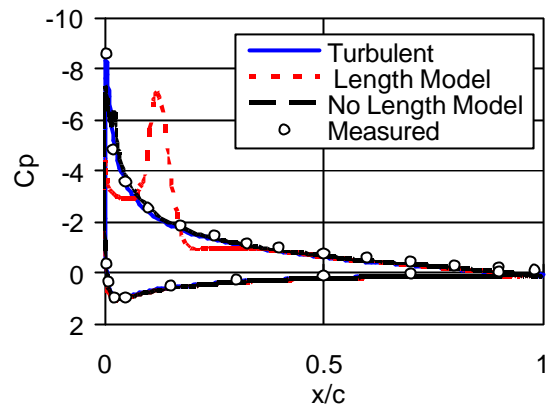


(b) Drag Coefficient

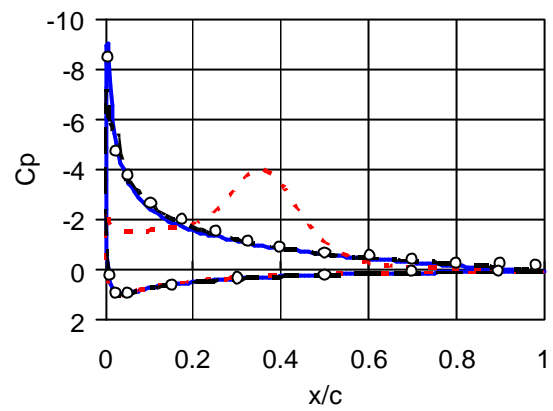


(c) Pitching Moment Coefficient

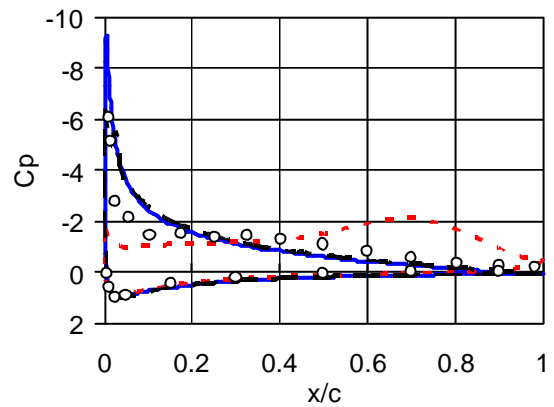
Figure (13) Influence of transition length on computed forces and moments for pitching aerofoil (fully attached transitional flow)



(a) $a(t) = 13.0^\circ$ (up stroke)



(b) $a(t) = 14.0^\circ$



(c) $a(t) = 13.0^\circ$ (down stroke)

Figure (14) Comparison of computed and measured pressure distributions for pitching aerofoil (separated flow)

intermittency was set to $c(x)=1$ immediately following the predicted transition location.

With this modification the computed pressure distributions appear to be in better agreement with the experimental data, Figure (14), than computations involving the use of the model.

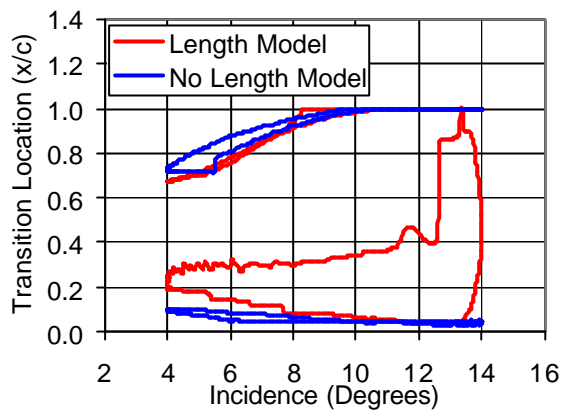


Figure (15) Influence of transition length on the predicted transition location for pitching aerofoil (fully attached transitional flow)

The influence of the transition length modelling on the predicted transition location is shown in Figure (15). Inclusion of a transitional region has a significant influence on the transition location. Without the use of the intermittency function the upper surface transition location remains close to the leading edge over the whole of the motion, this reflects more closely the expected behaviour from quasi-steady considerations. The computed forces and moments obtained without the length model are in much poorer agreement with the measured data.

Conclusions

A method for computing low Reynolds number flows containing laminar-turbulent transition has been described. The model employs empirical relationships to describe the onset and extent of transition and is coupled with a two equation turbulence model.

Results were presented for two aerofoil configurations that demonstrate the ability of the model to compute attached transitional flows and flows involving leading edge separation. Comparisons of the model predictions with experimental data were generally good. The computed upper and lower surface transition locations were acceptable while computed surface pressure, skin friction and boundary layer profiles all showed significant improvement compared to fully turbulent calculations.

For a fully attached unsteady flow the computed data showed only slight improvements over that obtained from

fully turbulent calculations. Comparison of the computed forces and moments with experimental data was generally favourable.

The use of the transition model for unsteady separating flows provides qualitative representations of the complex force and moment hysteresis observed experimentally that cannot be obtained with the assumption of fully turbulent flow. Quantitative agreement is generally poor during the down stroke with a much deeper stall predicted.

The predicted force and moment hysteresis was shown to be sensitive to both fixed transition location and transition length. The depth of the computed stall increases as the fixed transition point moves aft or as the transitional flow region is lengthened.

The movement of the upper surface transition location appears to be erroneous during the down stroke based upon quasi-steady considerations. This behaviour is attributed to deficiencies in the model relating the local velocity distribution to the computed pressure coefficients. Further work is required to improve this aspect of the model

Acknowledgements

The work described in this paper was supported by Westland Helicopters Ltd and the Engineering and Physical Science Research Council (EPSRC) within the HMB-UK consortium. Alan Brocklehurst (Westland Helicopters) was the technical monitor. The authors would like to acknowledge Professor Ian Poll for useful discussions and Professor D. Favier for granting permission for the use of the data generated at LABM, France.

References

1. Carr, L.W., 'Progress in Analysis and Prediction of Dynamic Stall', Journal of Aircraft, Vol. 25 (1), 1988, pp. 5-17.
2. Carr, L.W. and Chandrasekhara, M.S., 'Compressibility effects on Dynamic Stall', Progress in Aerospace Sciences, Vol. 32, pp. 523-573.
3. Beddoes, T.S., and Leishman, J.G., 'A semi-empirical model for dynamic stall', Journal of the American Helicopter Society, Vol. 34 (3), 1989.
4. Ekaterinaris, J.A., Srinivasan, G.R. and McCroskey, W.J., 'Present capabilities of prediction two-dimensional dynamic stall', Paper 2, AGARD CP 552, Berlin, 1994.
5. Ekaterinaris, J.A. and Platzer, M.F., 'Progress in Aerospace Science,
6. Malik, M.R., 'Boundary-layer transition prediction toolkit', AIAA-1997-1904.
7. Cebeci, T., 'Essential ingredients of a method for low Reynolds number airfoils', AIAA J., Vol. 27 (2), pp. 1680-88.

8. Ekaterinaris, J.A., Chandrasekhara, M.S. and Platzer, M.F., 'Analysis of low Reynolds number airfoil flows', *J. Aircraft*, Vol. 32 (3), pp. 625-630.
9. Michel, R., 'Etude de la transition sur les profile d'aile; Etablissement d'un critere de determination de point de transition et calcul de la trainee de profile incompressible', ONERA Report 1/1578A, 1951.
10. Hill, J.L., Shaw, S.T. and Qin, N., 'Engineering prediction of laminar/turbulent transition for isolated helicopter rotors in hover', Royal Aeronautical Society Aerodynamics Research Conference, London, September 2004.
11. Wilcox, D.C., 'Turbulence modelling for CFD', DCW Industries, 1993.
12. Osher, S. and Solomon, F., 'Upwind difference schemes for hyperbolic systems of conservation laws', *Mathematics of computation*, Vol. 38 (158), pp. 339-374.
13. Shaw, S.T. and Qin, N., 'Unsteady flow around helicopter rotor blade sections in forward flight', *The Aeronautical Journal of the Royal Aeronautical Society*, Vol. 103, pp. 35-44.
14. Qin, N., Ludlow, D.K. and Shaw, S.T., 'A matrix-free preconditioned Newton/GMRES method for unsteady Navier-Stokes solutions', *International Journal of Numerical Methods in Fluids*, Vol. 33, pp. 223-248.
15. Qin, N., Zhu, Y. and Shaw, S.T., 'Numerical study of active shock-control for transonic aerodynamics', *International Journal of Numerical Methods for heat and fluid flow*, Vol.14, No.4, 2004.
16. Qin, N., Ludlow, D.K., Shaw, S.T., Edwards, J.A., and Duquis, A. 'Calculation of pitch damping coefficients for a flared projectile', *J. Spacecraft and Rockets*, Vol. 34(4), 1997.
17. Thwaites, B., 'Approximate Calculation of the Laminar Boundary Layer', *Aeronautical Quarterly*, Vol 1, pp 245-280.
18. Krumbein, A., 'Transitional flow modeling and application to high-lift multi-element airfoil configurations', *J. Aircraft*, Vol. 40 (4), pp 786-794.
19. Schmidt, G. S., *Analysis of Low Reynolds Number Separation Bubbles Using Semi-empirical Methods*. AIAA J., Vol. 27 (8).
20. Walker, G.J., 'Transitional flow on axial turbomachinery blading', *AIAA J.*, Vol. 27 (5), pp. 595-602.
21. Wilcox, D.C., 'Simulation of transition with a two-equation turbulence model', *AIAA J.*, Vol. 32 (2), pp. 247-55.
22. Gregory, N. and O'Reilly, C.L., 'Low-speed aerodynamic characteristics of NACA 0012 aerofoil section, including the effects of upper-surface roughness simulating hoar frost', *NPL Aero Report 1308*, 1970.
23. Allain C. 'Contribution à l'étude expérimentale de la couche limite soumise à une instationnarité forcée. Application aux phénomènes de transition et de décollement en écoulement in stationnaire 2D/3D', PhD thesis, Université de la Méditerranée, 1999.
24. Favier D., Maresca C., Berton E., Allain C., 'Etude expérimentale et numérique du développement de la couche limite instationnaire sur modèles oscillants en écoulement 2D/3D.', DRET, Convention n°95-052, 1996.
25. Haase, W., Chaput, E., Elsholz, E., Leschziner, M.A. and Muller, U.R. (Editors), 'Validation of CFD codes and assessment of turbulence models', *Notes on numerical fluid mechanics*, Vol. 58, 1997.
26. Piziali, R.A., 'An experimental investigation of 2D and 3D oscillatory wing aerodynamics for a range of angle of attack including stall', *NASA TM 4632*, 1994.
27. McCroskey, W.J., 'The phenomena of dynamic stall', *NASA TM 81264*, 1981.